



# **Effects of Varying Load on DC- Link Voltage in DFIG Based Wind Energy Conversion System**

**Rakesh Sharma<sup>1</sup>, Kuldeep Sahay<sup>2</sup>, Sateyendra Singh<sup>3</sup>**

M.Tech. (Student), Uttar Pradesh Technical University, Lucknow, Uttar Pradesh, India<sup>1</sup>

Professor, Dept. of EE, Institute of Engineering & Technology, Lucknow, Uttar Pradesh, India<sup>2</sup>

Assistant professor, Dept. of EE, Institute of Engineering & Technology, Lucknow, Uttar Pradesh, India<sup>3</sup>

**ABSTRACT:** The wind energy sources are characterized by irregularity and unpredictability. It is very important to make DC-link voltage constant for doubly fed induction generator wind energy conversion system. The DC-link provides an extra spinning reserve facility for the wind system, which can be used for sink or source of active power. This paper presents the DC-link voltage fluctuation for a back to back pulse width modulation converter in doubly fed induction generator for wind turbine systems. The effects of load variation on DC link electrolytic capacitor voltage of DFIG based wind energy conversion system (WECS). As DFIG based WECS utilize low power converter, so there is a need to explore the effects of DC-link voltage. For this there are two cases (i) At fixed speed effect of load variation on dc link voltage  $V_{dc}$  (ii) At variable speed effect of load variation on dc link voltage  $V_{dc}$ . These cases are compared with healthy fixed and variable DFIG wind energy conversion system. All these scenarios have been simulated with the help of the simulation program using MATLAB and its inbuilt components provided in SIMULINK library.

**KEYWORDS:** Rotor Side Converter, Stator Side Converter, Pulse Width Modulation, Wound Rotor Induction Generator.

## **I. INTRODUCTION**

Over the last twenty years, renewable energy sources have been attracting great attention due to the cost increase, limited Reserves and adverse environmental impact of fossil fuels. In the meantime, technological Advancements, cost reduction, and Governmental incentives have made us to utilize more renewable energy sources for generation of electricity [1]. Wind energy is used for hundreds of Years for milling grains, pumping water, and sailing the seas. The use of windmills to generate electricity can be traced back to the late nineteenth century with the development of a 12kW dc windmill generator. It is, however, only since the 1980s that the technology has become sufficiently mature to produce electricity efficiently and reliably. Over the past two decades, a variety of wind power technologies have been developed, which have improved the conversion efficiency and reduced the costs for wind energy production. The size of wind turbine has increased from a few kilowatts to several megawatts each. In addition to on-land installation, larger wind turbines have been pushed to offshore location to harvest more energy and reduce their impact on land use and landscape [2]. With the increased penetration level of wind power in the power system, grid utilities want wind turbine generator system to behave like a conventional synchronous generator in terms of real and reactive power settings [3]. In other words, wind turbines have to contribute not only to active power generation but also to the reactive power. Hence, wind turbines should have extended reactive power capability not only during voltage dips but also in steady state operation [4]. Although, the DFIG wind turbines are able to control active and reactive power independently of one another by virtue of ac/dc/ac power electronic converter present on it, The grid side inverter reactive power capability can be taken into consideration, but in commercial system, this converter usually works with unity power factor, i.e. zero reactive power, so the total reactive power capability of the generator is equal to the stator reactive power capability [5, 6]. In [7], a rotor position Phase-Locked Loop (PLL) is used which acquires the rotor position and rotor speed simultaneously for the implementation of the decoupled P-Q control in the DFIG.



## International Journal of Advanced Research in Electrical, Electronics and Instrumentation Engineering

(An ISO 3297: 2007 Certified Organization)

Vol. 3, Issue 5, May 2014

### II. WIND TURBINE

Wind energy comes from wind turbine blades and then transferred to a gear box (to match the high speed generator with low speed turbine blades) & the rotor hub to provide mechanical energy to the shaft. The shaft drives the generator to convert the mechanical energy into electrical energy. The power of an air mass flowing at speed  $V$  through an area  $A$  can be calculated by

$$\text{Power} = \frac{\text{density of air} * \text{swept area} * \text{velocity cubed}}{2}$$

$$P = \frac{1}{2} \rho A V_w^3 \quad (1)$$

Where,  $P$  is power in watts (W),  $\rho$  is the air density in kilograms per cubic meter ( $\text{kg/m}^3$ ),  $A$  is the swept rotor area in square meter ( $\text{m}^2$ ),  $V$  is the wind speed in meter per second (m/s). But the turbine model is based on the power captured by the blade & converted into mechanical energy.

$$P_m = C_p (\lambda, \beta) \cdot \frac{1}{2} \rho A V_w^3 \quad (2)$$

$$\lambda = (R_{\text{blade}} \omega_r) / V_w$$

$$C_p (\lambda, \beta) = c_1 (c_2 - c_3 \beta - c_4 \beta^2 - c_5) e^{-c_6} \quad (3)$$

Where,  $c_1=0.5$ ,  $c_2=116/\lambda_i$ ,  $c_3=0.4$ ,  $c_4=0$ ,  $c_5=5$ ,  $c_6=21/\lambda_i$ ,

$$\frac{1}{\lambda_i} = \frac{1}{\lambda + 0.08 \beta} - \frac{0.035}{\beta^3 + 1} \quad (4)$$

Where  $P_M$  is the mechanical power output power in watts &  $C_p$  is the power coefficient of the blade which depends on the tip speed ratio ( $\lambda$ ) & blade pitch angle ( $\beta$ ).  $C_p$  decides how much energy can be captured by wind turbine system.

To get maximum  $C_p$ , one has blade pitch angle ( $\beta=0$ ) and tip speed ratio ( $\lambda=8$ ). In this paper wind turbine model, for different wind speeds and fixed pitch angle at  $\beta=0$ .

### III. DFIG WIND SYSTEM AND EQUATIONS

The DFIG is the same as the WRIG system except that variable resistance in the rotor circuit is replaced by a grid-connected power converter system & there is no need for the soft starter or reactive power compensation. And also the power factor is adjusted by power converter itself. The use of converters also allows bidirectional power flow in the rotor circuit & increase the speed range of the generator (extended generator speed range  $\pm 30\%$ ), also improved the overall power conversion efficiency. The DFIG typically operates about 30% above & below synchronous speed, sufficient for most wind speed conditions. It also enables generator side active power control & grid side active power control. In the DFIG model of wind energy the active and reactive power are controlled independently. The wind turbine drives DFIG wind system consists of a WRIG (wound rotor induction generator) and an AC/DC/AC IGBT based PWM converter (back to back converter with capacitor dc link) or we can say that two levels IGBT voltage source converter (VSC) system in a back to back configuration is normally used. Since both stator and rotor can feed power to grid, the generator is known as doubly fed induction generator (DFIG). It has two main parts, the rotor side converter control (RSC), which controls the torque or active/reactive power of the generator and, grid side converter controls (GSC), which controls the DC link voltage and its AC-side reactive power. An equivalent circuit of DFIG wind system shown in Fig.1 and Fig. 2a, 2b and relation equations to voltage  $V$ , current  $I$ , flux linkage  $\Psi$ , and electromagnetic torque  $T_e$  are as follows. Fig. 3 & 4 shows the rotor-side converter control of voltage block diagram and simulink model respectively and Fig. 5 shows the equivalent circuit of stator-side converter choke.

# International Journal of Advanced Research in Electrical, Electronics and Instrumentation Engineering

(An ISO 3297: 2007 Certified Organization)

Vol. 3, Issue 5, May 2014

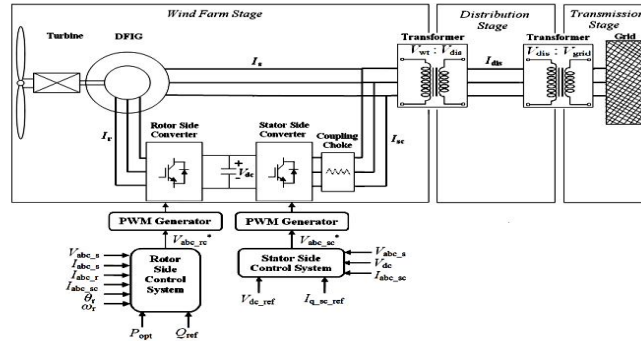


Fig.1 Wind Turbine DFIG System Configuration

d-q Reference frame model

Voltage equations

$$V_s = V_{ds} + j V_{qs} \tag{5}$$

$$I_s = I_{ds} + j I_{qs} \tag{6}$$

$$\Psi_s = \Psi_{ds} + j \Psi_{qs} \tag{7}$$

$$V_r = V_{dr} + j V_{qr} \tag{8}$$

$$I_r = I_{dr} + j I_{qr} \tag{9}$$

$$\Psi_r = \Psi_{dr} + j \Psi_{qr} \tag{10}$$

$$V_{ds} = R_s I_{ds} - \omega_s \Psi_{qs} + \frac{d\Psi_{ds}}{dt} \tag{11}$$

$$V_{qs} = R_s I_{qs} + \omega_s \Psi_{ds} + \frac{d\Psi_{qs}}{dt} \tag{12}$$

$$V_{dr} = R_r I_{dr} - s \omega_s \Psi_{ds} + \frac{d\Psi_{dr}}{dt} \tag{13}$$

$$V_{qr} = R_r I_{qr} + s \omega_s \Psi_{dr} + \frac{d\Psi_{qr}}{dt} \tag{14}$$

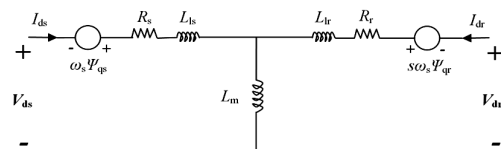


Fig. 2a d-axis Model

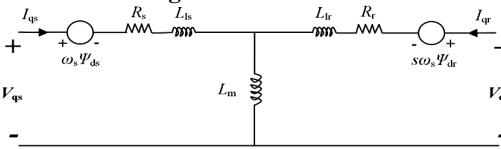


Fig. 2b q-axis Model

$$\Psi_{ds} = L_s I_{ds} + L_m I_{dr} \tag{15}$$

$$\Psi_{qs} = L_s I_{qs} + L_m I_{qr} \tag{16}$$

$$\Psi_{dr} = L_r I_{dr} + L_m I_{ds} \tag{17}$$

$$\Psi_{qr} = L_r I_{qr} + L_m I_{qs} \tag{18}$$

Electromagnetic torque equation

$$T_e = 3n_p / 2 (\Psi_{ds} I_{qs} - \Psi_{qs} I_{ds}) \tag{19}$$

Where  $L_s = L_{ls} + L_m$  \tag{20}

$$L_r = L_{lr} + L_m \tag{21}$$

$$s \omega_s = \omega_s - \omega_r \tag{22}$$

$$\Psi_{ds} = (V_{qs} - R_s I_{qs}) / \omega_s \tag{23}$$

$$\Psi_{qs} = (V_{ds} - R_s I_{ds}) / (-\omega_s) \tag{24}$$

$$\Psi_s = \sqrt{\Psi_{ds}^2} + \sqrt{\Psi_{qs}^2} \tag{25}$$

The subscripts r, s and d, q represents the rotor & stator, d-axis, q- axis components respectively,  $T_e$  is electromagnetic torque,  $L_m$  &  $J$  are generator mutual inductance, and the inertia coefficient, respectively.

# International Journal of Advanced Research in Electrical, Electronics and Instrumentation Engineering

(An ISO 3297: 2007 Certified Organization)

Vol. 3, Issue 5, May 2014

$$I_{dr\_ref} = -\frac{2L_s T_e}{3npL_m \Psi_s} \quad (26)$$

$$P_{ref} = P_{opt} - P_{loss} = T_e \omega_r \quad (27)$$

$$P_{loss} = R_s I_s^2 + R_r I_r^2 + R_c I_{sc}^2 + F \omega_r^2 \quad (28)$$

Where  $I_{sc}$ ,  $R_c$  and  $F$  are stator-side converter current & choke resistance, friction factor.  $P_{opt}$ ,  $P_{ref}$  and  $P_{loss}$  are desired optimal output active power, reference active power and system power loss.

$$Q_o = Q_s + Q_{sc} = Q_s \quad (29)$$

$$Q_o = \text{Im}[(V_{ds} + jV_{qs})(I_{ds} + jI_{qs})^*]$$

$$Q_o = -V_{ds} I_{qs}$$

$$Q_o = -V_{ds}(\Psi_s - L_m I_{qr}) / L_s \quad (30)$$

$$V_{dr}^2 = R_r I_{dr} - s\omega_s (L_r I_{qr} + L_m I_{qs}) \quad (31)$$

$$V_{qr}^2 = R_r I_{qr} + s\omega_s (L_r I_{dr} + L_m I_{ds}) \quad (32)$$

$$V_{drc} = V_{dr} = V_{dr}^1 + V_{dr}^2 \quad (33)$$

$$V_{qrc} = V_{qr} = V_{qr}^1 + V_{qr}^2 \quad (34)$$

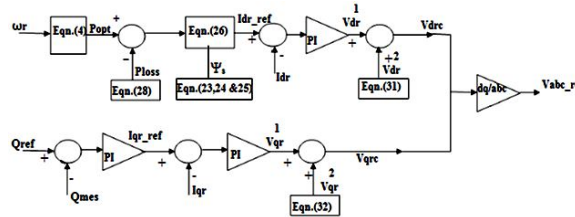


Fig. 3 Rotor-Side Converter Control Scheme ( $V_{abc\_rc}$ )

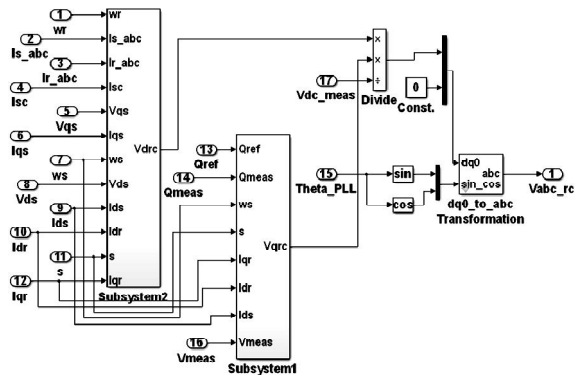


Fig.4 Simulink Model of Rotor-Side Converter Voltage ( $V_{abc\_rc}$ )

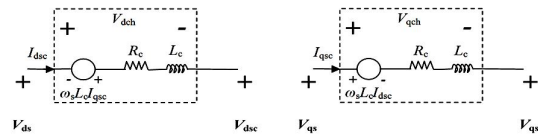


Fig.5 Equivalent Circuit of Stator Side Converter Choke

$$V_{dsc} = V_{ds} - V_{dch} \quad (35)$$

$$V_{qsc} = V_{qs} - V_{qch} \quad (36)$$

$$V_{dch}^2 = R_c I_{dsc} - \omega_s L_c I_{qsc} \quad (37)$$

$$V_{qch}^2 = R_c I_{qsc} + \omega_s L_c I_{dsc} \quad (38)$$

$$V_{dsc} = V_{ds} - V_{dch}^1 - V_{dch}^2 \quad (39)$$

$$V_{qsc} = V_{qs} - V_{qch}^1 - V_{qch}^2 \quad (40)$$

# International Journal of Advanced Research in Electrical, Electronics and Instrumentation Engineering

(An ISO 3297: 2007 Certified Organization)

Vol. 3, Issue 5, May 2014

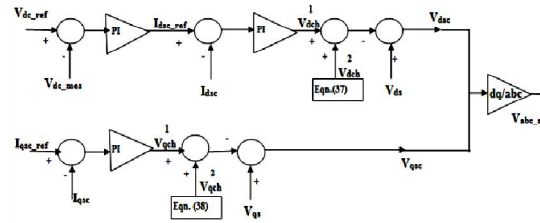


Fig.6 Stator-Side Converter Control Scheme

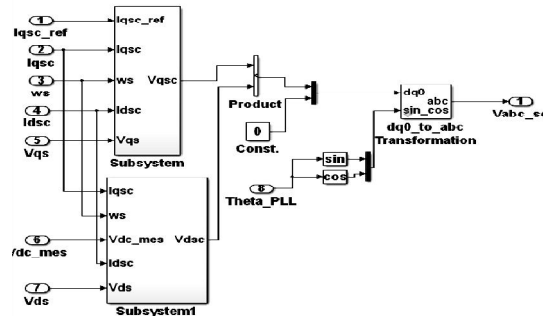


Fig.7 Simulink Model of Stator Side Converter Voltage  $V_{abc\_sc}$

Where the rotor-side converter voltage signals at q-axis  $V_{qr}^1$  and  $V_{qr}^2$  & at d-axis  $V_{dr}^1$  and  $V_{dr}^2$  are derived by regulation of currents and cross-coupling part.  $I_{dr\_ref}$  is the rotor-side converter reference current signals,  $V_{dch}^1$  and  $V_{qch}^1$  is the coupling part of voltage,  $V_{dch}^2$  and  $V_{qch}^2$  are determined by regulation of current  $I_{dsc}$  and  $I_{qsc}$  in which the current reference  $I_{qsc\_ref}$  is given directly while  $I_{dsc\_ref}$  is determined by the regulation of dc-link voltage  $V_{dc}$ .  $V_{dsc}$  and  $V_{qsc}$  is stator-side converter voltage signals. Fig. 6 & 7 shows the stator-side converter control of voltage block diagram and simulink model respectively. Fig. 9 shows the complete connection diagram of control blocks (rotor-side control and stator-side control).

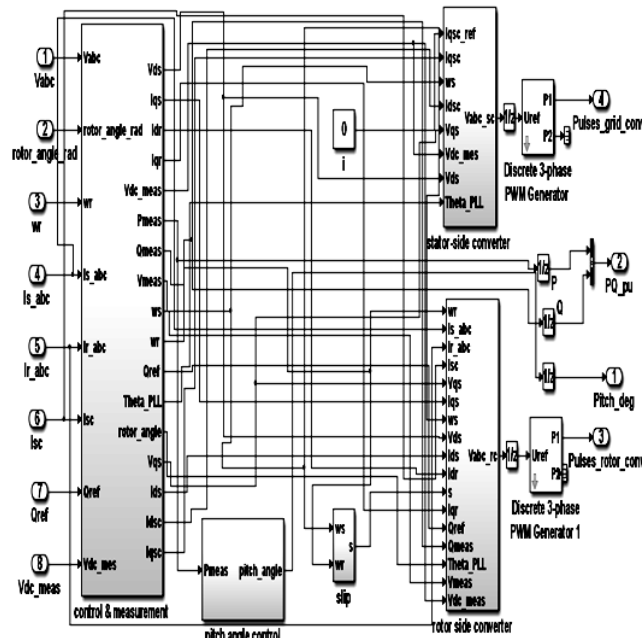


Fig.9 Connection Diagram of Control Blocks (RSC and SSC)

# International Journal of Advanced Research in Electrical, Electronics and Instrumentation Engineering

(An ISO 3297: 2007 Certified Organization)

Vol. 3, Issue 5, May 2014

## IV. SIMULINK MODELLING OF DFIG WIND SYSTEM

Fig. 10 shows DFIG wind model simulation in MATLAB/SIM-POWER SIMULINK. The three phase programmable source is generating power at 120 kV, which is stepped down to 25 kV by the two winding transformer and then transmitted by the 30 km long transmission line for further stepping down the voltage level to the 575 V at point of common coupling between grid and DFIG wind energy conversion system . The DFIG wind energy conversion system is generating power of 1.5 MW.

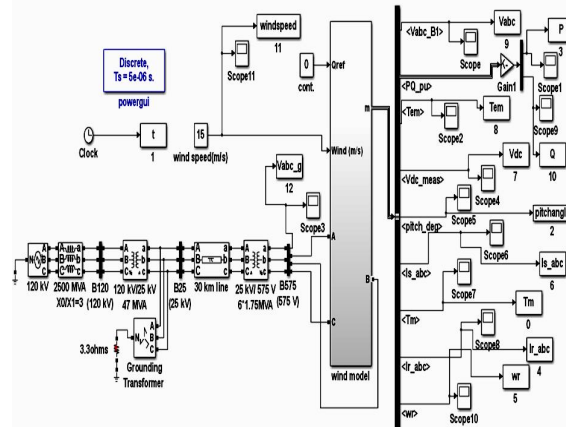


**Fig. 10 Development Test Model for DFIG Wind System**

In this, the wind turbine uses a doubly-fed induction generator (DFIG), which consists of a wound rotor induction generator and an AC/DC/AC IGBT-based PWM converter. The dc voltage is applied to IGBT/Diode's of two level inverter. The pulse width modulation technique has been used in this inverter, in order to achieve higher accuracy , the carrier frequency or switching frequency is 1620 Hz, discrete sample time is,  $T_s = 5$  microseconds. The stator winding is connected directly to the 60 Hz grid while the rotor is fed at variable frequency through the AC/DC/AC converter. The DFIG wind system allows extracting maximum energy from the wind for low wind speeds by optimizing the turbine speed, while minimizing mechanical stresses on the turbine during the gusts of wind. In this, wind speed is maintained constant at 15 m/s. The DC voltage is regulated at 1200 V and reactive power is kept at 0 Mvar. When we double click on wind model block then it shows a generator, a converter, a turbine, & a drive train and the control system block.

### (A) DFIG WORKING ANALYSIS AT FIXED SPEED

#### DC link Voltage, Grid Side voltage without and with Filter ( $V_{dc}$ , $V_{abc\_g}$ , $V_{abc}$ )

Fig 11, Fig 12 & Fig 13 shows the grid voltage with and without filter and dc link voltage under the fixed wind speed. It can be seen that the voltage  $v_{abc}$ ,  $v_{abc\_g}$  has little-bit variation during starting up to 0.4 sec and after that it will become stable & maintained constant at 0.6 pu, the dc link voltage  $V_{dc}$  almost constant during simulation time (1.2 sec).

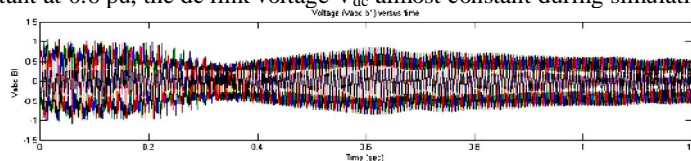


**Fig. 11 Voltage ( $V_{abc}$ ) versus Time**

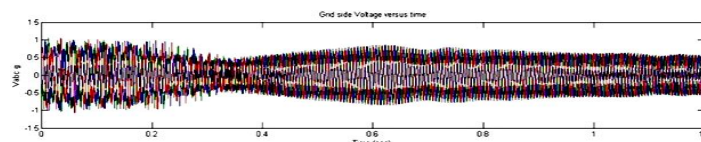


**Fig. 12 Grid-Side Voltage ( $V_{abc\_g}$ ) versus Time**



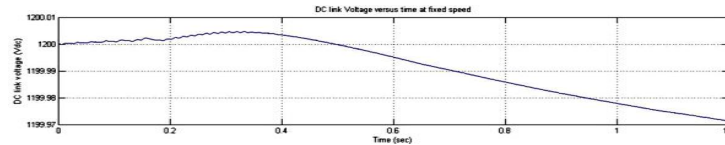


**Fig. 13 DC Link Voltage ( $V_{dc}$ ) versus Time**

### Stator and Rotor Current of DFIG

Fig 14 & Fig.15 shows the stator-side and rotor-side current of DFIG wind system under fixed wind speed. It can be seen that rotor current of DFIG system has variation between 0.5 to 0.6 sec and between 0.9 to 1.1 sec and beside these point it is almost constant which is almost 1 pu and little above but the stator current has less variation between 0.5 to 0.6 sec and between 0.9 to 1.1 sec as compare to rotor current beside these points it is almost stable.

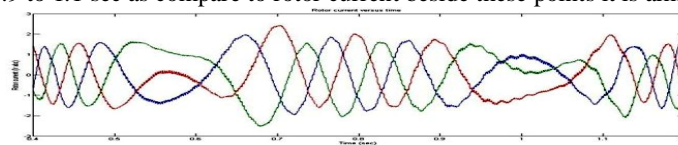


**Fig. 14 Rotor Side Current ( $I_{r\_abc}$ ) versus Time**

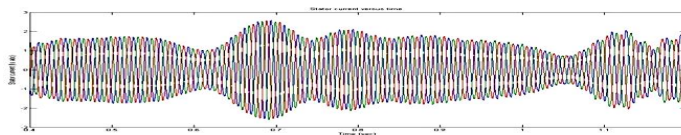


**Fig. 15 Stator Side Current ( $I_{s\_abc}$ ) versus Time**

### Active and Reactive Power Variation

Fig. 16 And 17 shows the active and reactive power of DFIG wind energy system under fixed wind speed. It can be seen that the active power varies around the required 1.5 MW, the average variation in the real power and reactive power is almost negligible. Fig. 17 shows that during period 0.6 to 0.7 sec it is supplying reactive demanded by load while during period 0.7 to 0.75 sec the reactive power is being absorbed by system.

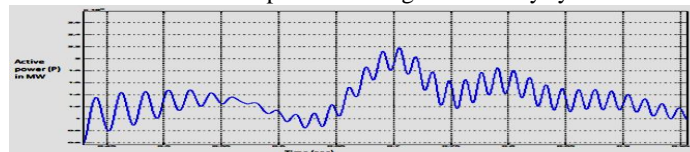


**Fig. 16 Active Power (P) versus Time**

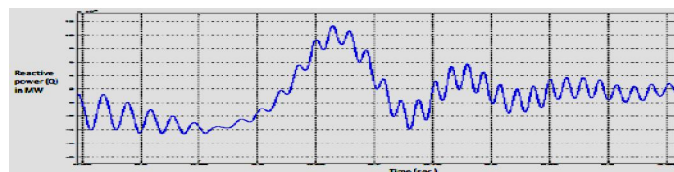


**Fig. 17 Reactive Power (Q) versus Time**

### Variation of Electro-Mechanical Torque Developed Torque ( $T_{em}$ and $T_m$ )

Fig. 18 shows the Electro-Mechanical Torque ( $T_{em}$ ) under the fixed wind speed. It can be seen that the torque is Pulsating but the torque during starting of the simulation are very low, while developed torque ( $T_m$ ) are smooth.

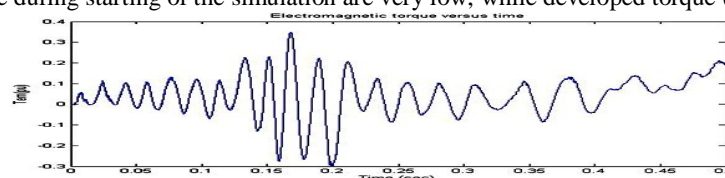


**Fig. 18 Electro-Mechanical Torque ( $T_{em}$ ) Versus Time**

# International Journal of Advanced Research in Electrical, Electronics and Instrumentation Engineering

(An ISO 3297: 2007 Certified Organization)

Vol. 3, Issue 5, May 2014

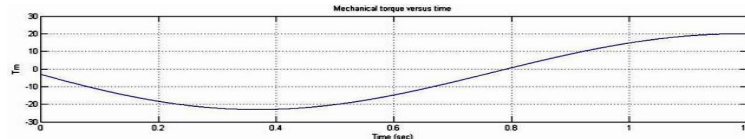


Fig. 19 Mechanical Torque ( $T_m$ ) versus Time

## (B) DFIG SYSTEM PARAMETER ANALYSIS AT VARIABLE SPEED

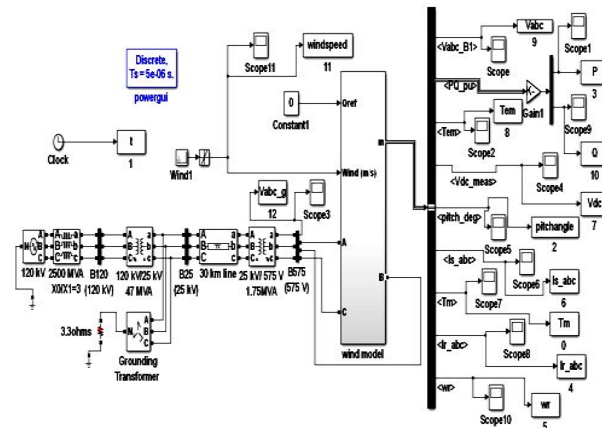


Fig. 24 Simulink Diagram of DFIG Wind

## ENERGY CONVERSION SYSTEM AT VARIABLE SPEED

### DC link Voltage, Grid Side voltage without and with Filter ( $V_{dc}$ , $V_{abc_g}$ , $V_{abc}$ )

Fig. 24, 25 and Fig. 26 shows the Grid Side voltage without and with Filter, DC link Voltage, ( $V_{abc}$ ,  $V_{abc_g}$ ,  $V_{dc}$ ). It can be seen that the variation of voltage  $V_{abc}$  and  $V_{abc_g}$  are very much with respect time in comparison to fixed wind speed system. But the  $V_{dc}$  developed almost constant. The dc link voltage has a little bit variation. In case with filter the becomes quite smooth.

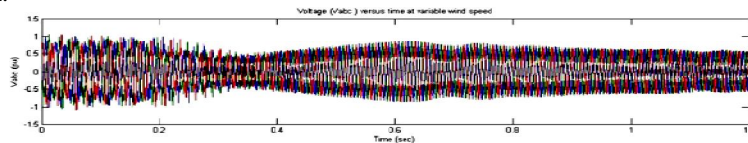


Fig. 25 Grid Side Voltage with Filter ( $V_{abc}$ ) versus Time

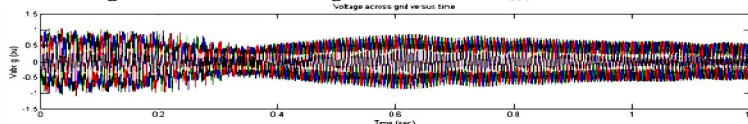


Fig. 26 Grid Side voltage without Filter ( $V_{abc_g}$ ) versus time

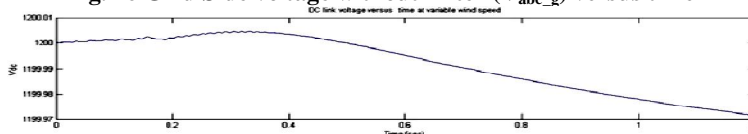


Fig. 27 DC Link Voltage ( $V_{dc}$ ) versus Time

### Stator and Rotor Current of DFIG

Fig. 28 and 28 shows the stator and rotor current of DFIG wind system at variable wind speed. It can be seen that rotor current of DFIG system has variation between 0.5 to 0.6 sec and between 0.9 to 1.1 sec and beside these point it is almost constant, which is almost 1 pu but the stator current has less variation between 0.5 to 0.6 sec and between 0.9 to 1.1 sec



# International Journal of Advanced Research in Electrical, Electronics and Instrumentation Engineering

(An ISO 3297: 2007 Certified Organization)

Vol. 3, Issue 5, May 2014

1.1 sec as compared to rotor current, beside these points it is almost stable. But the variations in currents with respect time are more in comparison to fixed wind speed system.

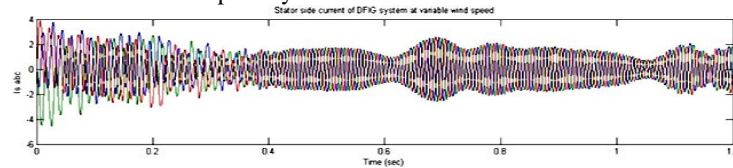


**Fig. 28 Stator Side Current (I<sub>s\_abc</sub>) versus Time**

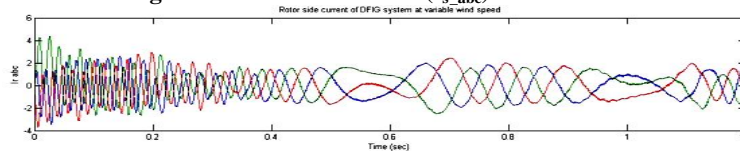


**Fig. 29 Rotor Side Current (I<sub>r\_abc</sub>) versus Time**

### Active and Reactive Power variation

Fig. 30 and 31 shows the active and reactive power of DFIG wind energy system under variable wind speed. It can be seen that the both active power and reactive power has little variation as compare to fixed wind speed system. Fig. 31 shows some time it gives power and some time it absorbs the power (reactive power with respect time curve). Compare to fixed speed the variable speed system working is quite better.

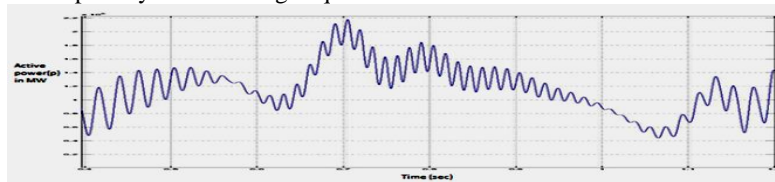


**Fig. 30 Active Power (P) versus Time at Variable Wind Speed**

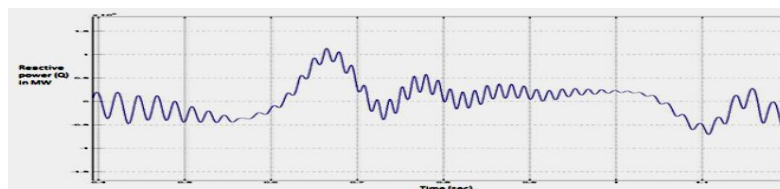


**Fig. 31 Reactive Power (Q) versus Time at Variable Wind Speed**

### Variation of Electro-Mechanical Torque and Developed Torque (T<sub>em</sub> and T<sub>m</sub>)

Fig. 32 & 33 shows the Electro-Mechanical Torque (T<sub>em</sub>) & developed torque (T<sub>m</sub>). T<sub>em</sub> has little bit variation in comparison to the fixed speed and after 0.7 sec. it is varying. But developed torques' T<sub>m</sub> are smooth.

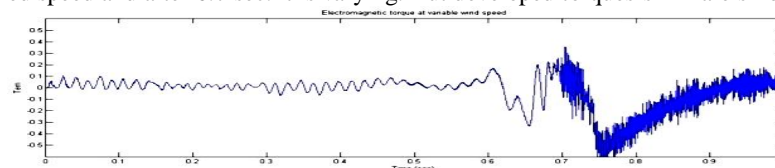


**Fig. 32 Electro-Mechanical Torque (T<sub>em</sub>) versus Time**

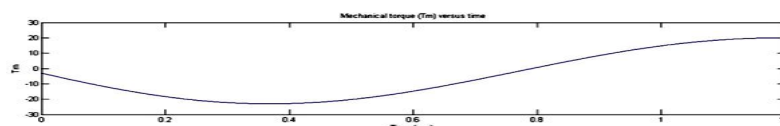


**Fig. 33 Wind Turbine Developed Torque (T<sub>m</sub>) versus Time**

# International Journal of Advanced Research in Electrical, Electronics and Instrumentation Engineering

(An ISO 3297: 2007 Certified Organization)

Vol. 3, Issue 5, May 2014

## CASE:-1 SIMULATION RESULTS WHEN THE FIXED WIND SPEED IS PASSED ON DFIG (C) AT FIXED SPEED EFFECT ON DC LINK VOLTAGE $V_{dc}$

### Effect on DC Link Voltage when the load is 1.5 Mw Load

The developed simulink model in Figure No. 35 was simulated for 2 sec at the load of 1.5 MW at the fixed speed of 15 m/s during simulation. it can seen in Fig. 34 the dc link voltage ( $V_{dc}$ ) up to 0.43 sec it is almost constant and after 0.43 sec there is variation the dc link voltage of only 0.05 volts up to 1.83 sec. The value of dc link voltage is 1199.95 volt at that point. Practically the  $V_{dc}$  developed can be considered constant.

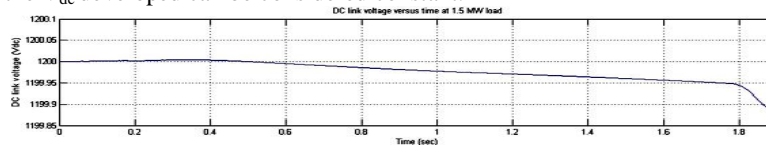


Fig. 34 DC Link Voltage versus Time at 1.5 MW Load (Fixed Speed)

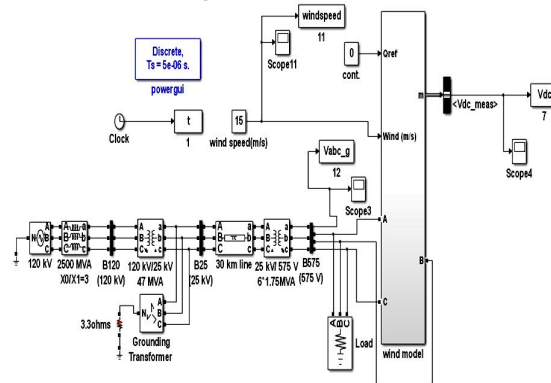


Fig. 35 Simulink Diagram during Loading at Bus B575 at Fixed Wind Speed

### Effect on DC Link Voltage when the load is 1 Mw Load

Fig. 36 shows the DC link voltage ( $V_{dc}$ ) at 1MW load. The developed simulink model was simulated for 2 sec at the load of 1 MW at the fixed of 15 m/s during simulation .it can seen that the dc link voltage up to 0.43 sec it is almost constant and after 0.43 sec there is variation the dc link voltage of only 0.05 volts but it is decreases after 1.85 sec. The value of dc link voltage is 1199.95 volt, which can practically very much closure to 1200 V.

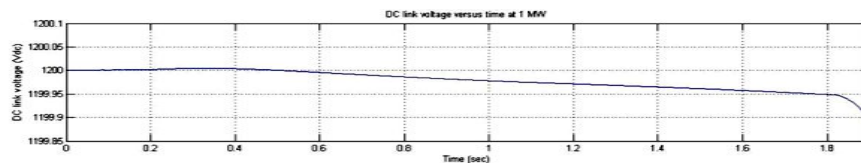


Fig. 36 DC Link Voltage versus Time at 1 MW Load (Fixed Speed)

### Effect on DC Link Voltage when the load is 0.5 Mw Load

Fig. 37 shows the DC link voltage ( $V_{dc}$ ) at 0.5MW load under fixed wind speed. The developed simulink model was simulated for 2 sec at the load of 0.5 MW at the fixed of 15 m/s during simulation .it can seen that the dc link voltage up to 0.43 sec it is almost constant and after 0.43 sec there is variation the dc link voltage of only 0.05 volts but it is decreases after 1.87 sec. The value of dc link voltage is 1199.95 volt. Which can practically very much closure to 1200 Volt.

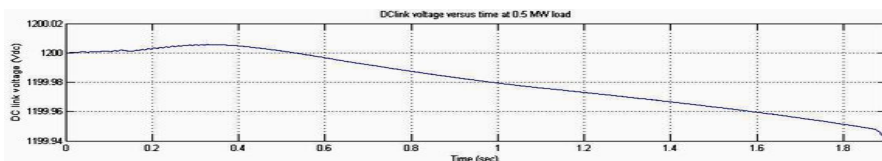


Fig. 37 DC Link Voltage versus Time at 0.5 MW Load (Fixed Speed)

# International Journal of Advanced Research in Electrical, Electronics and Instrumentation Engineering

(An ISO 3297: 2007 Certified Organization)

Vol. 3, Issue 5, May 2014

## CASE:-2 SIMULATION RESULTS WHEN THE VARIABLE WIND SPEED IS PASSED ON DFIG

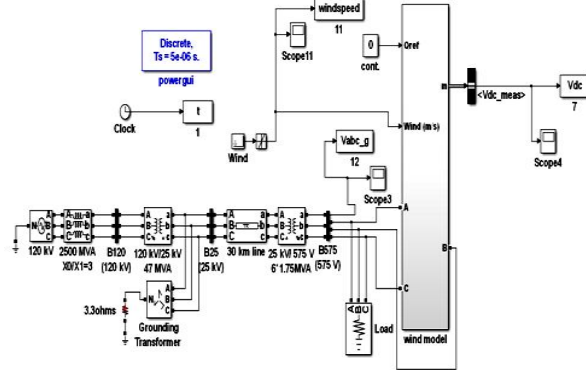


**Fig. 38 Simulink Diagram during Loading at Bus B575 for a Variable Wind Speed (D) AT VARIABLE SPEED EFFECT ON DC LINK VOLTAGE  $V_{dc}$**

### Effect on Dc Link Voltage at 1.5 MW Load

The developed simulink model in Figure No.38 was simulated for 2 sec in the Fig. 39 the DC link voltage ( $V_{dc}$ ) at 1.5MW load under variable wind speed i.e. 12 to 15 m/s was simulated at 1.5 MW, during simulation .It can be seen that the dc link voltage up to 0.58 sec it is almost constant .However after 0.58 sec there is variation the dc link voltage of only 0.05 volts but it decreases after 1.79 sec. up to 1.83. The value of dc link voltage is 1199.95 volt at that point.

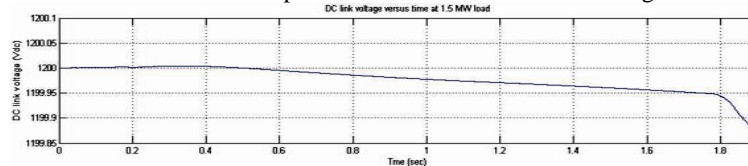


**Fig. 39 DC Link Voltage versus Time at 1.5 MW Load (Variable Speed)**

### Effect on Dc Link Voltage at 1.0 MW Load

Fig. 40 shows the DC link voltages ( $V_{dc}$ ) at 1.0 MW load under variable wind speed. The developed simulink model was simulated for 2 sec at the load of 1.0 MW at the variable wind speed from 12 to 15 m/s during simulation .it can be seen that the dc link voltage up to 0.58 sec it is almost constant and after 0.58 sec there is variation the dc link voltage of only 0.05 volts but it decreases after 1.854 sec. The value of dc link voltage is 1199.95 volt.

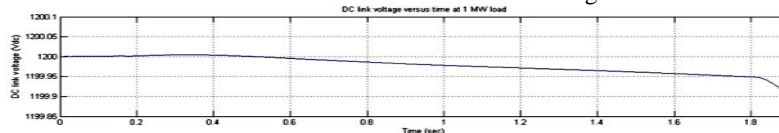


**Fig. 40 DC Link Voltage versus Time at 1.0 MW Load (Variable Wind Speed)**

### Effect on Dc Link Voltage at 0.5 MW Load

Fig. 41 shows the DC link voltage ( $V_{dc}$ ) at 0.5MW load under variable wind speed. The developed simulink model was simulated for 2 sec at the load of 0.5 MW at the variable wind speed from 12 to 15 m/s during simulation .it can be seen that the dc link voltage up to 0.58 sec it is almost constant and after 0.58 sec there is variation the dc link voltage of only 0.001 volts but it decreases after 1.675 sec. The value of dc link voltage is 1199.999 volt at that point. So, here it can say that fix speed wind system are good for dc link voltage to connect the load at grid end.

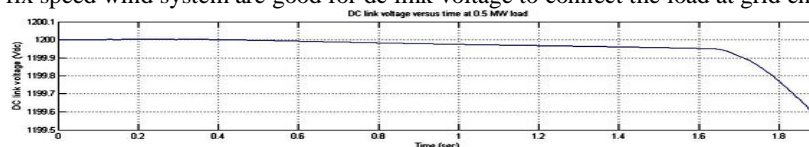


**Fig. 41 DC Link Voltage versus Time at 0.5 MW Load (Variable Wind Speed)**



# International Journal of Advanced Research in Electrical, Electronics and Instrumentation Engineering

(An ISO 3297: 2007 Certified Organization)

Vol. 3, Issue 5, May 2014

## VI. CONCLUSION

A DFIG wind system have been modelled and simulated in MATLAB software. It can be seen that when DFIG wind system is operated without load at both fixed and variable speed the DC-link voltage are almost constant. But when the DFIG wind system are loaded with different load at grid-side for fixed wind speed ,then it can be seen that as the load of the system is decreases the DC-link voltage remains constant more time than the higher load. However in case increase in the load there in very nominal effect on the load link voltage profile. But when the DFIG wind system are loaded with varying load at grid system for variable wind speed, it can be seen that when the 1.5MW load is applied DC-link voltage is almost constant 1.79 s.& for 1MW load it is almost constant up to 1.825s.,and for 0.5 MW load it is almost constant up to 1.63s.,it is observes that for variable wind speed system the dc-link voltage is very much constant in compare with fixed speed system .But the main difference between variable and fixed wind speed system is that when the load goes lower beyond certain level the dc link voltage stability gets affected while in fix speed there is no effect on the stability. So it is here concluded that whenever DFIG system is operated there should a minimum load on the system for getting constant DC link voltage.

## REFERENCES

- [1]. Renewable Energy Policy Network for the 21<sup>st</sup> Century (REN21), available at [www.ren21.net](http://www.ren21.net).
- [2]. T.Burton, D.Sharpe, N.Jenkins and E.Bossanyi, Wind energy handbook, Wiley, 2001.
- [3]. Stephan Engelhardt, Istvan Erlich, Christian Feltes, Jörg Kretschmann, and Fekadu Shewarega, "Reactive Power Capability of Wind Turbines Based on Doubly Fed Induction Generator," IEEE Trans. on Energy Conversion, Vol. 26, No. 1, pp. 364-372, March 2011.
- [4]. Mustafa Kayıkçı and Jovica V. Milanović, "Reactive Power Control Strategies for DFIG-Based Plants," IEEE Trans. on Energy Conversion, Vol. 22, No. 2, pp. 389-396, June 2007.
- [5]. Torsten Lund, Poul Sorenson and Jarle Eek, "Reactive Power Capability of a Wind Turbine with Doubly Fed Induction Generator," Wind Energy, vol. 10, iss. 4, pp.379-394, Apr. 2007.
- [6]. D. Santos-Martin, S. Arnaltes, and J.L. Rodriguez-Amenedo, "Reactive power capability of doubly fed asynchronous generators," Electric Power Systems Research, vol.78, pp.1837-1840, 2008.
- [7]. Bakari Mwinyiwiwa, Yongzheng Zhang, Baike Shen, and Boon-Teck Ooi, "Rotor Position Phase-Locked Loop for Decoupled P-Q Control of DFIG for Wind Power Generation," IEEE Transactions on Energy Conversion, vol. 24, no. 3, pp. 758-765, Sept. 2009.
- [9] Cortajarena J.A., De Marcos J., Alvarez P., Vicandi F.J. Alkorta P., "Start up and control of a DFIG wind turbine test rig", IECON 2011 - 37th Annual Conference on IEEE Industrial Electronics Society, Nov 2011.
- [10]. R. R. Peters, D. Muthumuni, T. Bartel, H. Salehfar, and M. Mann, "Dynamic Model Development of a Fixed Speed Stall Control Wind Turbine at Start-Up", Power Engineering Society General Meeting, IEEE, 2006.
- [11]. Ankit Gupta, S.N.Singh, Dheeraj K. Khatod, "Modeling and Simulation of Doubly Fed Induction Generator Coupled with Wind Turbine –An Overview", JEC&AS, Vol. 2, No.8, Aug. 2013.
- [13]. Jun Yao, Hui Li, Yong Liao, and Zhe Chen, "An Improved Control Strategy of Limiting the Dc-Link Voltage Fluctuation for a Doubly Fed Induction Generation", IEEE Transactions on Power Electronics, Vol.23, No.3, May 2008.
- [15]. S. N. Singh, Jacob Østergaard, and Bharat Singh, "Reactive Power Capability of Unified DFIG for Wind Power Generation", IEEE, 2010.

## BIOGRAPHY



**Rakesh Sharma** is a M. Tech student in the Department of Electrical Engineering, Institute of Engineering & Technology, Lucknow. He received his B.Tech degree in Electrical Engineering from Sagar Institute of Technology & Management, Barabanki, India, in 2007. He has total 04 years of teaching experience in IET (as a contractual faculty), Lucknow. His research area of interest includes DFIG wind energy conversion system, fault analysis and performance enhancement.



**Kuldeep Sahay**, Ph.D. is associated with Institute of Engineering & Technology, Lucknow since 1996, where, he is presently Professor in the Department of Electrical Engineering, An Autonomous Constituent College of Gautam Buddha Technical University (Formerly Uttar Pradesh Technical University), Lucknow. He has authored numbers of research paper in National and International Journal having good citation and published a book. His research interests are in the area of Mathematical Modeling of Energy Storage System, Integration of Renewable Energy System with Grid. Prof. Sahay for his overall contribution in research and academics has been awarded "Shiksha Rattan Puraskar" and "Rashtriya Gaurav Award" by India International Friendship Society, New Delhi in 2011



**Satyendra Singh, M. Tech.** is associated with Institute of Engineering & Technology, Lucknow since 2008, where, he is presently Assistant Professor in the Department of Electrical Engineering, An Autonomous Constituent College of Gautam Buddha Technical University (Formerly Uttar Pradesh Technical University), Lucknow. He has authored numbers of research paper in National and International Journal having good citation. His research interests are in the area of power systems.